

# Enzymatic Synthesis of Phloretin $\alpha$ -Glucosides Using a Sucrose Phosphorylase Mutant and its Effect on Solubility, Antioxidant Properties and Skin Absorption

Jose L. Gonzalez-Alfonso,<sup>a, b</sup> Zorica Ubiparip,<sup>b</sup> Elena Jimenez-Ortega,<sup>c</sup> Ana Poveda,<sup>d</sup> Cristina Alonso,<sup>e</sup> Luisa Coderch,<sup>e</sup> Jesus Jimenez-Barbero,<sup>d, f</sup> Julia Sanz-Aparicio,<sup>c</sup> Antonio O. Ballesteros,<sup>a</sup> Tom Desmet,<sup>b,\*</sup> and Francisco J. Plou<sup>a,\*</sup>

<sup>a</sup> Institute of Catalysis and Petrochemistry (ICP-CSIC), 28049 Madrid, Spain

Tel: +34-915854869

E-mail: fplou@icp.csic.es

<sup>b</sup> Centre for Synthetic Biology (CSB), Department of Biotechnology, Ghent University, 9000 Ghent, Belgium

Tel. +32-92649920

E-mail: tom.desmet@ugent.be

<sup>c</sup> Institute of Physical-Chemistry Rocasolano, CSIC, 28006 Madrid, Spain

<sup>d</sup> Center for Cooperative Research in Biosciences, CIC bioGUNE, Basque Research & Technology Alliance, BRTA, 48160 Derio, Biscay, Spain

<sup>e</sup> Institute of Advanced Chemistry of Catalonia (IQAC-CSIC), 08034 Barcelona, Spain.

<sup>f</sup> Ikerbasque, Basque Foundation for Science, Plaza Euskadi 5, 48009 Bilbao, Spain

Manuscript received: February 12, 2021; Revised manuscript received: April 15, 2021;

Version of record online: ■■, ■■■



Supporting information for this article is available on the WWW under <https://doi.org/10.1002/adsc.202100201>

© 2021 The Authors. Advanced Synthesis & Catalysis published by Wiley-VCH GmbH. This is an open access article under the terms of the Creative Commons Attribution Non-Commercial NoDerivs License, which permits use and distribution in any medium, provided the original work is properly cited, the use is non-commercial and no modifications or adaptations are made.

**Abstract:** Glycosylation of polyphenols may increase their aqueous solubility, stability, bioavailability and pharmacological activity. Herein, we used a mutant of sucrose phosphorylase from *Thermoanaerobacterium thermosaccharolyticum* engineered to accept large polyphenols (variant TtSPP\_R134A) to produce phloretin glucosides. The reaction was performed using 10% (v/v) acetone as cosolvent. The selective formation of a monoglucoside or a diglucoside (53% and 73% maximum conversion percentage, respectively) can be kinetically controlled. MS and 2D-NMR determined that the monoglucoside was phloretin 4'-O- $\alpha$ -D-glucopyranoside and the diglucoside phloretin-4'-O-[ $\alpha$ -D-glucopyranosyl-(1 $\rightarrow$ 3)-O- $\alpha$ -D-glucopyranoside], a novel compound. The molecular features that determine the specificity of this enzyme for 4'-OH phenolic group were analysed by induced-fit docking analysis of each putative derivative, using the crystal structure of TtSPP and changing the mutated residue. The mono- and diglucoside were, respectively, 71- and 1200-fold more soluble in water than phloretin at room temperature. The  $\alpha$ -glucosylation decreased the antioxidant capacity of phloretin, measured by DPPH and ABTS assays; however, this loss was moderate and the activity could be recovered upon deglycosylation *in vivo*. Since phloretin attracts a great interest in dermocosmetic applications, we analyzed the percutaneous absorption of glucosides and the aglycon employing a pig skin model. Although the three compounds were detected in all skin layers (except the fluid receptor), the diglucoside was present mainly on superficial layers.

**Keywords:** Phloretin; enzymatic glycosylation; polyphenol bioavailability; glucosides; skin absorption; glycoside phosphorylases

## Introduction

Living organisms are continually subjected to endogenous and exogenous oxidants that can damage their biomolecules such as DNA, lipids and proteins. These oxidative physiological processes can derive in disorders like cancer, Alzheimer disease, Parkinson disease, arthritis, cardiovascular problems or inflammation.<sup>[1]</sup> Even at low concentrations, antioxidants can inactivate intracellular Reactive Oxygen Species (ROS) and other free radicals.<sup>[2]</sup> Among them, plant polyphenols have demonstrated a notable efficiency against these disorders.<sup>[3]</sup>

Phloretin (2',4',6'-trihydroxy-3-(4-hydroxyphenyl)-propiophenone) is a dihydrochalcone mainly present in most parts of apple trees – including the skin and pomace of apples –,<sup>[4]</sup> which possesses a notable antioxidant activity and stands out for a variety of biological properties. Thus, it displays an inhibitory effect on the active transport of glucose,<sup>[5]</sup> which makes it an interesting compound as antidiabetic. Hsiao et al. demonstrated the phloretin capacity to suppress cancer cells invasion and migration, acting as a potential anticancer assistant combined with other current treatments.<sup>[6]</sup> The inhibition of a HIV-1 transmembrane protein by phloretin and its  $\beta$ -glucoside derivative trilobatin was also reported.<sup>[7]</sup>

The low aqueous solubility of phloretin (<0.2 mM) constrains its applications in functional food and pharmaceutical industries.<sup>[8]</sup> This fact is well related to its low bioavailability, manifested in a low oral absorption, fast metabolism, and rapid elimination in the urine and feces.<sup>[9]</sup> Apart from pharmaceutical strategies (formation of complexes with cyclodextrins, nanosuspensions, etc.) or absorption boosters,<sup>[10]</sup> the modification of the structure of polyphenols by glycosylation is an excellent way to increase their hydrophilicity and stability, leading to an improved bioavailability and better pharmacological activity.<sup>[11]</sup>

In nature, we can find many polyphenol glycosides, e.g. bearing a glucose, rhamnose or arabinose residue.<sup>[12]</sup> The sugar moiety can play an important role in intestinal absorption<sup>[13]</sup> and bioavailability.<sup>[14]</sup> Furthermore, the glycosylation of polyphenols can modulate their pharmacokinetic properties, stability and solubility in comparison with the aglycon.<sup>[15]</sup>

To obtain polyphenol glycosides, the use of enzymes offers several advantages over chemical processes.<sup>[16]</sup> Glycosyl hydrolases (GHs)<sup>[17]</sup> can serve that purpose but typically offer low yields of glycosylated derivatives.<sup>[18]</sup> Transglycosidases (TGs) display a higher transfer to hydrolysis ratio and employ cheap donor substrates such as sucrose or maltodextrins.<sup>[16,19]</sup> Glycosyltransferases (GTs) offer the highest yields by far, but they require expensive nucleotide-activated sugar donors.<sup>[20]</sup>

In this context, glycoside phosphorylases have attracted increasing attention as biocatalysts for glycosyl transfer.<sup>[21]</sup> *In vivo*, they catalyze the degradation of di- and oligosaccharides with inorganic phosphate, but the reaction is readily reversible *in vitro* due to the high energy content of the synthesized glycosyl phosphate.<sup>[22]</sup> Interestingly, sucrose phosphorylases (SPs) can also be used as transglycosidases as they are able to transfer the glucosyl unit of sucrose to different acceptors such as oligosaccharides, phenolic derivatives or alkyl glucosides.<sup>[23]</sup> Nevertheless, the activity of SPs using bulky phenolic compounds as acceptors is rather limited.

Several enzyme engineering strategies have been developed to increase the acceptor specificity of glycosidic enzymes for large polyphenolic compounds, including SPs and related enzymes.<sup>[15b,24]</sup> Dirks-Hofmeister et al. reported the R134A mutant of sucrose 6'-phosphate phosphorylase from *Thermoanaerobacterium thermosaccharoliticum* (TtSPP\_R134A),<sup>[25]</sup> which exhibits higher affinity for polyphenols than the native enzyme, caused by the increased size of the catalytic pocket. The mutant was active towards more than 80% of the phenolic compounds assayed as glucose acceptors, including the bulkiest phenolics.<sup>[25]</sup> In particular, it was effective for the glucosylation of a variety of polyphenols such as pyrogallol, methyl gallate, ethyl gallate, propyl gallate, lauryl gallate, resveratrol, quercetin, catechin or epicatechin.<sup>[26]</sup>

In the present work, we report the synthesis of phloretin glucosides using the sucrose phosphorylase mutant TtSPP\_R134A. The products were chemically characterized and some of their properties (antioxidant activity, solubility, etc.) assayed in comparison with the aglycon. In particular, the effect of glucosylation on skin absorption was studied since one of the current applications of phloretin is in dermatologic formulations.<sup>[27]</sup>

## Results and Discussion

### Phloretin Glucosylation

Phloretin glucosylation was investigated using the R134A mutant of the sucrose 6'-phosphate phosphorylase from *T. thermosaccharoliticum* (TtSPP\_R134A). The reaction was carried out in 50 mM MOPS buffer (pH 6.5) containing 10% (v/v) acetone to increase the phloretin solubility, using an excess of sucrose (1 M) with regard to polyphenol (5 mg/mL).

The reaction was followed by Thin Layer Chromatography (TLC). Two new spots appeared on the TLC plate, which could correspond to glucosylated derivatives. The formation of three products was observed by HPLC (Figure 1): one major peak (Glc-Phloretin-1) and two minor peaks (Glc-Phloretin-2 and -3). However, the concentration of Glc-Phloretin-2 became

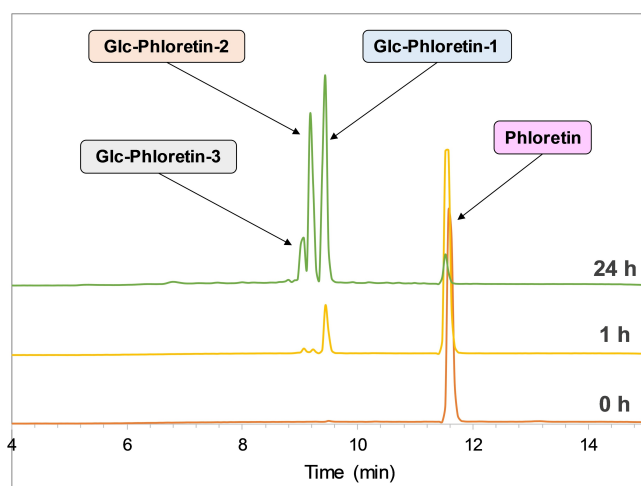


**Figure 1.** HPLC chromatogram of the phloretin glucosylation reaction at 48 °C after 0 h, 1 h and 24 h. Reaction conditions: phloretin (5 mg/mL), sucrose (342 mg/mL), MOPS buffer (50 mM, pH 5.6), acetone (10% v/v) and TtSPP\_R134A (5 U/mL).

significant at the latter stages of the reaction, in contrast with Glc-Phloretin-3.

The progress of the formation of the two main reaction products was determined (Figure 2). As shown, the synthesis of the first product (Glc-Phloretin-1) reaches its maximum (4.2 mg/mL, 53% conversion yield) after approximately 12 h (the remaining phloretin is almost negligible at that time), and then it decreases with time alongside the appearance of the second product (Glc-Phloretin-2). The concentration of this second product stabilizes at about 8 mg/mL (73% conversion yield). The conversion of phloretin into its

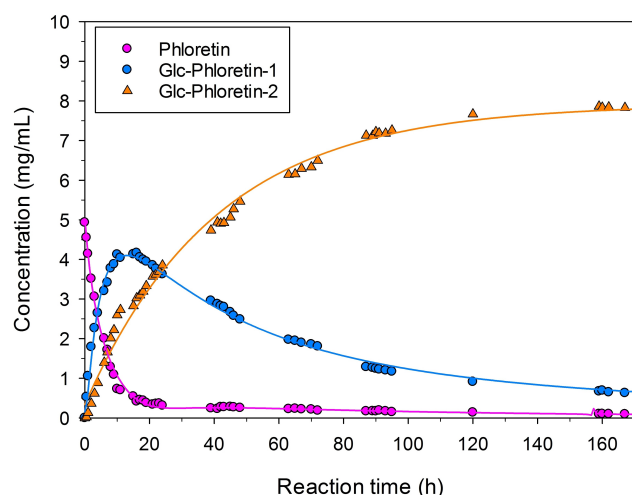


**Figure 2.** Kinetics of the formation at 48 °C of the two characterized phloretin glucosides. Reaction conditions: phloretin (5 mg/mL), sucrose (342 mg/mL), MOPS buffer (50 mM, pH 5.6), acetone (10% v/v) and TtSPP\_R134A (5 U/mL).

glucosides is really efficient compared with similar glucosylations of related polyphenols catalyzed by GHs and TGs, in which the reported conversion yields are substantially lower.<sup>[12,28]</sup>

Most of the glycosylation studies on phloretin have been carried out with GTs employing UDP-sugar donors, yielding the C-glucoside nothofagin<sup>[29]</sup> or the  $\beta$ -glucoside at 2'-OH phlori(d)zin.<sup>[30]</sup> To our knowledge, the only work on phloretin glucosylation using GHs was performed by Overwin et al. using the amylosucrase from *Neisseria polysaccharea*.<sup>[31]</sup> Starting from 10 mM phloretin (half of the concentration employed in the present work), they synthesized a mixture of a mono-, di- and tri-glucoside with conversion efficiency of 35%, 32% and 28%, respectively. However, the process described herein catalyzed by the mutant TtSPP\_R134A allows directing the reaction selectively to the mono- or the di-glucoside (Figure 2).

### Characterization of Glucosides

The reaction was scaled up to 20 mL and the main products were purified by silica gel chromatography as described in the Experimental Section. Both products (Glc-Phloretin-1 and Glc-Phloretin-2) were characterized by ESI-MS and NMR.

Their molecular weights were determined by ESI-MS coupled to a QTOF analyzer in positive mode. For Glc-Phloretin-1 we observed the presence of a major peak with  $m/z$  459.1264 that corresponded to the ion  $[M+Na]^+$  of the monoglucoside (Figure S1, Supplementary Material). In the case of Glc-Phloretin-2, we observed the major peak with  $m/z$  of 621.1787, which fitted with the  $[M+Na]^+$  ion of the diglucoside (Figure S2, Supplementary Material).

The glucosylation position of the monoglucoside sample (Glc-Phloretin-1) was determined by NMR. 1D-selective TOCSY and NOESY experiments, complemented by 2D-HSQC and 2D-HMBC spectra, were performed to identify and assign the signals. Two similar compounds were detected in the mixture in a 1:13 ratio. Both compounds exhibit an anomeric proton with  $J=3.7$  Hz, indicative of an  $\alpha$  linkage. For the major compound, the anomeric H1'' of glucose showed NOE correlation with 3'-H and 5'-H aromatic protons of B ring (Figures S3-A and S3-B, Supplementary Material), which demonstrated  $\alpha$ -glucosylation at 4'-O position of such ring. This arrangement was also confirmed by a HMBC correlation connecting Glc-H1'' to C4'. Therefore, the structure of the major glucoside **1** is represented in Figure 3. The same glucoside structure has been reported by Overwin et al. using the amylosucrase from *Neisseria polysaccharea*.<sup>[31]</sup>

In contrast, for the minor compound (8%), the corresponding anomeric proton H1'' showed NOE

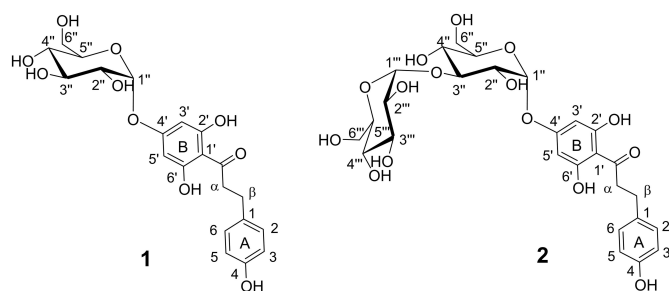


**Figure 3.** Chemical structures of the two major phloretin glucosides obtained. (1) Phloretin 4'-O- $\alpha$ -D-glucopyranoside, for the monoglucosylated sample Glc-Phoretin-1; (2) Phloretin 4'-O-[ $\alpha$ -D-glucopyranosyl-(1 $\rightarrow$ 3)-O- $\alpha$ -D-glucopyranoside], for the diglucosylated sample Glc-Phoretin-2.

correlation with one of the aromatic protons of the ring A, indicating that, in this case, glucosylation took place at position 4-OH of this ring (Figure S3-B, Supplementary Material).

With respect to the diglucoside fraction (Glc-Phoretin-2), the NMR spectra revealed a more complex mixture of products. The major one displayed two anomeric signals (H1'' and H1''') with similar J coupling values, ca. 3.7 Hz (corresponding to  $\alpha$ -Glc linkages). The <sup>1</sup>H signals for these two Glc residues could be determined by using COSY and 1D-selective TOCSY experiments. The connectivity of these residues was determined by using 1D-selective ROESY experiments, which showed NOE correlation between H1''  $\alpha$ -Glc and ring B. The other Glc moiety showed NOE between H1''' and H3''' of the Glc unit linked to the phloretin moiety (Figure S4, Supplementary Material). This H3''' correlates in the <sup>1</sup>H-<sup>13</sup>C HSQC spectrum with a <sup>13</sup>C signal at  $\delta$  84.3 ppm, typical for a glycosidation position (Figure S5, Supplementary Material). Thus, the proposed structure for compound 2 is phloretin 4'-O-[ $\alpha$ -D-glucopyranosyl-(1 $\rightarrow$ 3)-O- $\alpha$ -D-glucopyranoside], which is also represented in Figure 3.

To the best of our knowledge, the diglucoside 2 is a novel compound. In fact, for the diglucoside reported by Overwin et al. with amylosucrase, the glucoses were  $\alpha$ (1 $\rightarrow$ 4) linked. The main properties of the two synthesized derivatives are summarized in the Experimental Section.

### Docking Analysis of TtSPP\_R134A Structure in Complex with Different Phloretin Monoglucosylated Products

We tried to decipher the molecular features that determine the outstanding specificity of mutant TtSPP\_R134A to  $\alpha$ -glucosylate the 4'-OH of phloretin, which could be useful to modulate the enzyme specificity by enzyme engineering tools.<sup>[32]</sup> We per-

formed induced-fit docking analysis of each putative derivative using as template the crystal structure of TtSPP after modelling the Arg134 to Ala replacement (considering the PDB sequence with 14 residues long N-terminal polyhistidine-tag, Arg134 corresponds to Arg148 in the deposited coordinates). Thus, three different phloretin monoglucosylated ligands were built considering the glycosylation to occur at *para*- and *ortho*- positions in the triphenolic ring, or at the phenolic hydroxyl group.

The first run of docking analysis using Autodock 4.2<sup>[33]</sup> revealed that the best results were obtained for the *p*-glucosylated compound at the triphenolic ring, in which near half of the calculated conformations (within 2.0 Å root mean square) converged in the minimum binding energy of  $-7.5$  kcal/mol (Figure S6, Supplementary Material), whilst the two other derivatives gave more dispersed solutions among less populated clusters, with minimum binding energies of  $-4$  and  $-6.5$  kcal/mol, respectively. This observation was in accordance with the fact that the 4'- derivative was the main glucosylated product determined by NMR.

To go deeper into molecular interactions that govern the specificity of this reaction, AutoDock Vina was used to explore different modelling approaches.<sup>[34]</sup> In order to improve the accuracy of the docking method, Phe146, Phe171, Tyr215, Glu252, His358, which are delineating the catalytic tunnel and are therefore key residues in acceptor-substrate binding, were defined as flexible side chain residues. Around 20 solutions were calculated in a binding energy range between  $-12.6$  and  $-11.6$  kcal/mol. From these, conformers were selected based on their minimum energy and more conservative interactions at subsite  $-1$  (Figure 4A), which was checked by comparison to the reported complex of the homologous *Bifidobacterium adolescentis* sucrose phosphorylase with sucrose (BaSP, PDB code 2GDV).<sup>[35]</sup> Thus, the glucose moiety binds at subsite  $-1$ , with Arg209 (O2), His309 (O3), Asp63 (O4, O6) and His101 (O6), making polar links to the glucose hydroxyls, as previously described in that complex and other sucrose related complexes (Figure 4A).<sup>[23b]</sup>

An inspection of the modeled conformers showed that the open cavity defined by the R148A mutation delineates a long tunnel in which the phloretin moiety is allocated through hydrophobic interactions of the triphenolic ring, which is sandwiched between His358, on one side, and Phe171 and Tyr215, on the other (Figure 4B). Thus, main differences observed among the different solutions obtained from the docking analysis are found in the position of the terminal phenolic ring, which can adopt different orientations, possibly through stacking to Phe146 side-chain, which is located at the beginning of the flexible loop Lys144-Tyr153.

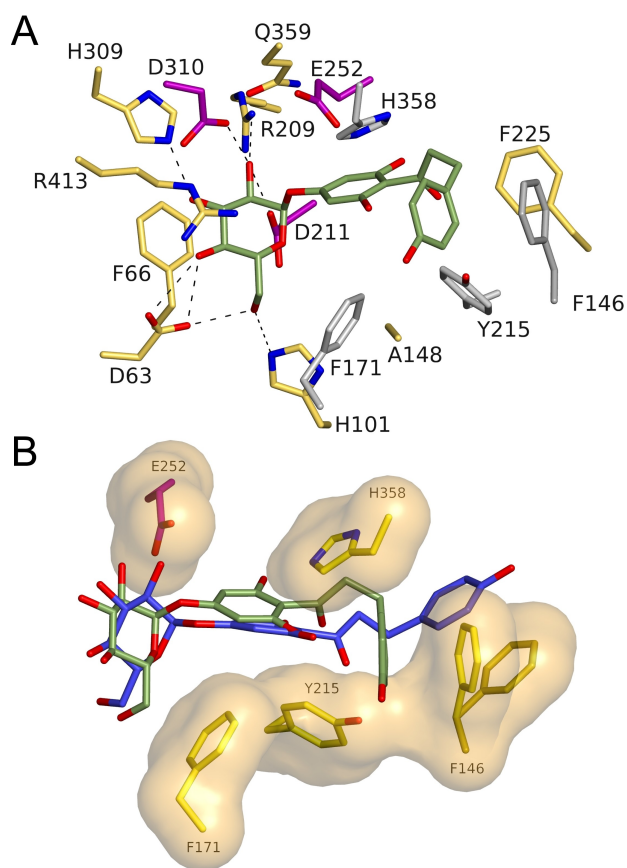


**Figure 4.** Docking simulation of mono-glucosylated phloretin into the TtSPP\_R134A mutant. **(A)** Interactions of a representative conformer of the first-ranked cluster in the catalytic pocket of TtSPP, as a result of the final docking simulation from AutoDock Vina. The catalytic residues are shown in purple, and residues defined as flexible are represented in grey, except the catalytic Glu252. **(B)** The residues considered flexible in the calculation do not move significantly and constrict binding of the triphenyl moiety of phloretin, allowing mobility only at the terminal phenyl ring. Two conformers are represented to highlight the conformational changes observed at the Phe146 side-chain, which modulate the position of the terminal phenyl.

In conclusion, docking simulations predict an efficient  $\alpha$ -glycosylation of the phloretin molecule at *para*- position (4'-), with a rather constrained location of the triphenol moiety of the acceptor, which is more accessible to the catalytic pocket by removal of the bulky Arg148 side-chain.

### Effect of Glycosylation on Phloretin Solubility

Glycosylation is a practical approach to increase the solubility (and thus the bioavailability) of lipophilic polyphenols.<sup>[36]</sup> In particular, we reported the synthesis of pterostilbene  $\alpha$ -monoglucoside using a cyclodextrin glucosyltransferase (CGTase) from *Thermoanaerobacter sp.*<sup>[37]</sup> Although the pterostilbene is almost

insoluble in water, the glucosylated derivative displayed a solubility of  $98 \pm 2$  mg/L. In this context, the anomeric configuration of the glycosyl moiety may exert a notable influence on the solubility properties. We demonstrated that  $\alpha$ -glucosylation of resveratrol increased its solubility 65-fold, whereas  $\beta$ -glucosylation in the same position (piceid) was only 12-fold more soluble.<sup>[38]</sup> This effect on solubility had also an impact on the surfactant activity of such compounds.

In the present work, we analyzed the solubility of phloretin and its glucosides, at 25 °C. The concentration of each compound after 72 h is summarized in Table 1. Interestingly, the  $\alpha$ -monoglucosylation caused a 71-fold increase in the aqueous solubility of phloretin. The effect of diglycosylation was even more pronounced (1200-fold increase). In contrast, in the presence of 10% (v/v) acetone, the solubility of phloretin was only ten times higher than in water.

### Effect of Glycosylation on Antioxidant Properties

The antioxidant activity of the  $\alpha$ -glucosides obtained from phloretin was analyzed with two different methods (using ABTS $\bullet^+$  and DPPH as radicals) and compared with the aglycon. Figure 5 shows the Trolox Equivalent Antioxidant Capacity (TEAC) values of the phloretin and its glucosides. A value lower than 1 means that the compound possesses more antioxidant capacity than Trolox on ABTS $\bullet^+$  (Figure 5A) or DPPH (Figure 5B) reduction.

As shown in Figure 5, the  $\alpha$ -glucosylation decreases the antioxidant capacity of phloretin with a statistically significant difference. This effect was expected since the antioxidant mechanism of polyphenols is related to the presence of OH groups that can donate a hydrogen to another compound. The decrease upon glucosylation has been observed with related compounds such as resveratrol.<sup>[38]</sup> However, the loss of antioxidant capacity is not very large and initial activity could be recovered upon deglycosylation *in vivo*.<sup>[39]</sup>

**Table 1.** Solubility of phloretin and glucosylated products at 25 °C.

Compound	Solubility (g/L)
Phloretin <sup>[a]</sup>	$0.023 \pm 0.001$
Phloretin <sup>[b]</sup>	$0.207 \pm 0.009$
Phloretin 4'- <i>O</i> - $\alpha$ -D-glucopyranoside ( <b>1</b> ) <sup>[a]</sup>	$1.6 \pm 0.2$
Phloretin 4'- <i>O</i> -[ $\alpha$ -D-glucopyranosyl-(1 $\rightarrow$ 3)- <i>O</i> - $\alpha$ -D-glucopyranoside] ( <b>2</b> ) <sup>[a]</sup>	$27.8 \pm 0.4$

<sup>[a]</sup> In water.

<sup>[b]</sup> In MOPS (50 mM) at pH 6.5 containing 10% (v/v) of acetone.

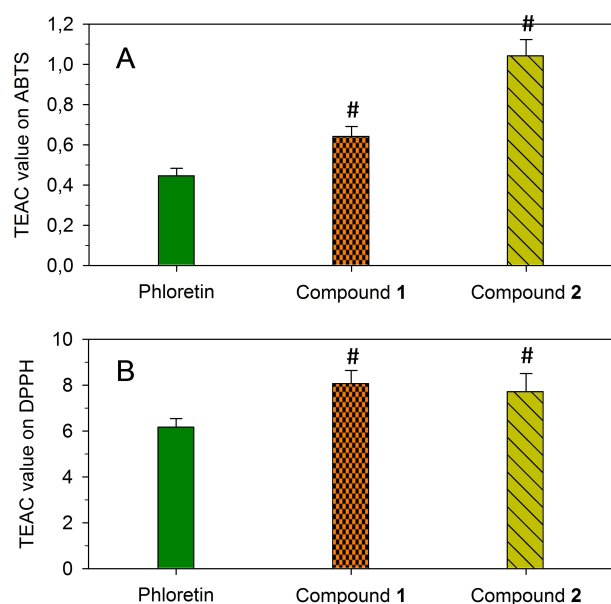


**Figure 5.** Antioxidant effect of phloretin and its glucosides on (A) ABTS<sup>•+</sup> reduction and (B) DPPH reduction. In the assay, Trolox was used as reference. Data is expressed as TEAC value  $\pm$  SD ( $n=3$ , # indicates  $p < 0.025$  vs. phloretin).

### Effect of Glucosylation on Percutaneous Absorption

Phloretin has great potential in cosmetic application because of its capacity to protect cells against UV radiation and/or antimicrobial activity.<sup>[27,40]</sup> In this context, we analyzed the percutaneous absorption using pig skin placed in a vertical diffusion cell as model (Figure S7, Supplementary Material).<sup>[41]</sup> The resulting recovery was acceptable ( $100 \pm 15\%$ ) for all the tested solutions. The amount of compound present in different skin layers was analyzed by HPLC (Figure 6). The amounts retained by the stratum corneum were not absorbed by the skin and do not contribute to the systemic dose. Percutaneous absorption (Perc. Abs) is assumed to be the sum of compound amount present in epidermis, dermis and receptor fluid (Figure S8, Supplementary Material).

All compounds were detected in all skin layers except the fluid receptor. Phloretin showed its ability to penetrate to the innermost layers of the skin (detected at dermis level) due to its high lipophilicity ( $\log P > 2$ ) and low molecular weight. Glycosylation of phloretin (monoglucoside) showed a penetration profile similar to phloretin, without significant differences. Therefore, monoglucoside, even being more hydrophilic due to derivatization, provides a greater antioxidant action in the same skin layers as phloretin. In addition, the stratum corneum layer can act as a reservoir, retaining these compounds and maintaining their antioxidative effect for longer.

However, the diglucoside, with highest molecular weight and hydrophilicity, is detected mainly in super-

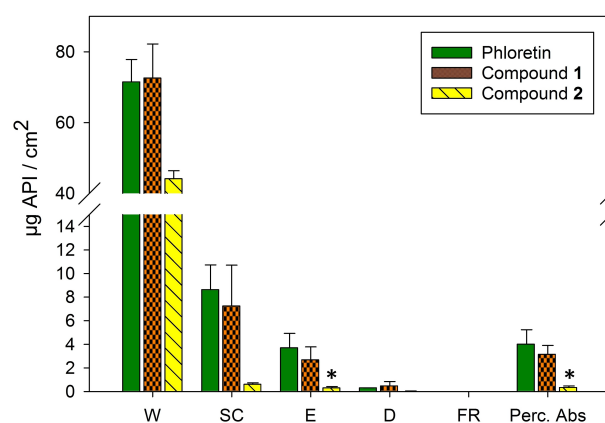


**Figure 6.** Skin distribution of phloretin, its monoglucoside (1) and diglucoside (2) within the different skin layers. W is the surface excess, SC is the stratum corneum, E is the epidermis, D is the dermis, FR is the fluid receptor and Perc. Abs. is the percutaneous absorption. The results were expressed as  $\mu\text{g/cm}^2$  (mean values  $\pm$  standard deviations,  $n=3$ , \* $p < 0.05$ ) of Active Pharmaceutical Ingredient (API).

ficial layers. This fact could make the diglucosylated derivative an interesting compound for cosmetic applications, which require compounds with moderate antioxidant capacity and low skin absorption to protect the skin surface for longer time periods.<sup>[42]</sup> The higher solubility of both derivatives provides an advantage for the preparation of the dermocosmetic formulations.

### Conclusion

This article demonstrates that phloretin glucosylation can be achieved with a high conversion efficiency by using the phosphorylase mutant TtSPP\_R134A. The glucosylation position of the monoglucoside was determined by 2D-NMR and the structural features that determine this specificity were deciphered by a docking model. A novel phloretin diglucoside was synthesized, in which the glucoses are bound by an unusual  $\alpha(1 \rightarrow 3)$  linkage. Although the synthesized glucosides display less antioxidant activity compared with the aglycon, their greater aqueous solubility could increase the bioavailability. In addition, the diglucoside showed a lower skin penetrability, which could be useful for cosmetic preparations due to its capacity to protect external skin layers over a prolonged time. Glycosylation of phloretin could become a strategy to obtain a prodrug for pharmaceutical preparations with a better uptake compared to the aglycon.

## Experimental Section

### Materials

Phloretin was purchased from Hunan MT Health Inc. (Hunan, China). Sucrose was obtained from Scharlau. BCA (2,2-Biquinoline-4,4-dicarboxylic acid dipotassium salt trihydrate), ABTS [2,2'-azino-bis(3-ethylbenzothiazoline-6-sulphonic acid)], DPPH (2,2-diphenyl-1-picrylhydrazyl) and (R)-Trolox (6-hydroxy-2,5,7,8-tetramethylchroman-2-carboxylic acid) were acquired from Sigma Aldrich. All other reagents and solvents were of the highest purity grade available.

### Enzyme Production

For the production of recombinant sucrose phosphorylase mutant TtSPP\_R134A from *Thermoanaerobacterium thermo-saccharolyticum*, the encoding gene was ligated into the expression plasmid pCXshP34 as described in previous works.<sup>[33]</sup> Next, the plasmid was transformed into *E. coli* BL21 cells. To produce the enzyme, the cells were grown at 37 °C (with continuous shaking at 200 rpm) in 5 mL of LB medium with 5  $\mu$ L of ampicillin (100 mg/mL) during 8 h. Next, the preculture was added to 500 mL of LB medium contained in a 2 L Erlenmeyer flask with 500  $\mu$ L of ampicillin. The culture was grown overnight at 37 °C with continuous shaking at 200 rpm. Subsequently, the cells were centrifuged at 10,000 rpm and 4 °C during 15 min, and the cell pellet was frozen at -20 °C. To extract the enzyme from the cells, the frozen cell pellet was slowly thawed on ice, and the cells were suspended in lysis buffer, containing lysozyme (1 mg/mL) and 1% of 10 mM phenylmethanesulfonyl fluoride (PMSF) in 50 mM MOPS buffer at pH 6.5. The suspended cells were subsequently disrupted by sonication (Branson 250 Sonifier, level 3, 50% duty cycle) 3 times during 3 min each cycle. The cell debris was removed by centrifugation for 30 min at 4,000 rpm and 4 °C, and the supernatant (crude cell extract) containing the enzyme was collected. The enzyme was semi-purified using heat purification, by incubating the crude cell extract in a water bath at 60 °C during 30 min. After this step, the mixture was centrifuged at 4,000  $\times$  g during 30 min and the supernatant was recovered and stored at 4 °C.

### BCA Assay for Protein Concentration

The protein concentration was determined using the Pierce™ BCA Protein Assay Kit (Thermo Fisher Scientific), following the manufacturer's instructions. For the calibration curves, bovine serum albumin standard (BSA) solution was provided with the kit.

### Assay for Enzyme Activity

The sucrose phosphorylase activity was evaluated by the bicinchoninic acid (BCA) assay for reducing sugars described by Waffenschmidt et al. with some modifications.<sup>[43]</sup> This assay was adapted to a 96-well microplate scale. The BCA solution was prepared as a mixture of stock solutions A, B and ethanol (100%) in the ratio 23:1:6. Stock solution A contained 1.56 g/L of 4,4'-dicarboxy-2,2'-biquinoline dipotassium salt (Sigma-Aldrich) and 62.3 g/L of anhydrous Na<sub>2</sub>CO<sub>3</sub> (Fluka). Stock

solution B was composed out of 3.5 g aspartic acid (Sigma-Aldrich) and 5 g of anhydrous Na<sub>2</sub>CO<sub>3</sub> (Fluka) dissolved in 100 mL of ultra-pure water, which was subsequently mixed with 1.09 g of CuSO<sub>4</sub> (Riedel-de Haën) dissolved in 40 mL of ultra-pure water. Additional water was then added to a total volume of 150 mL for the final B solution. A calibration standard curve of fructose between 0 and 250  $\mu$ M was made. The reaction mixture (1 mL) contained 200 mM phosphate and 100 mM sucrose in 50 mM MOPS buffer (pH 6.5). The enzyme (10  $\mu$ L) was conveniently diluted to fit into the calibration curve. The incubation was at 55 °C and samples were taken at different times during 14 min. Aliquots (25  $\mu$ L) and fructose standards were added to wells containing 150  $\mu$ L of BCA solution. The plate was covered and incubated at 70 °C for 30 min in the dark. The absorbance was measured with a spectrophotometer (Zenyth 200) at 540 nm. One unit of activity (1 U) corresponded to the release of one  $\mu$ mol of reducing sugars per minute.

### General Procedure for Phloretin Glucosylation

For the glucosylation reaction, 10 mg of phloretin in 200  $\mu$ L of acetone were mixed with 684 mg of sucrose in 1400  $\mu$ L of 50 mM MOPS buffer (pH 6.5) and 200  $\mu$ L of sucrose phosphorylase TtSP\_R134A (10 U). The total volume was 2 mL. The reaction was maintained at 48 °C during 24 h with orbital shaking (800 rpm) and followed by thin-layer chromatography (TLC) and high-performance liquid chromatography (HPLC). The TLC analysis was carried out with 60 F<sub>254</sub> silica gel plates (Merck) with a mixture of ethyl acetate, methanol and H<sub>2</sub>O (30:5:4) as mobile phase. The plate was revealed under UV light and using 10% of H<sub>2</sub>SO<sub>4</sub> solution. HPLC analysis was performed using a quaternary pump (model 600, Waters, Milford, MA, USA) coupled to an autosampler (model ProStar 420, Varian Inc., Palo Alto, CA, USA). The column was a Zorbax Eclipse Plus C18 (4.6  $\times$  100 mm, 3.5  $\mu$ m, Agilent) at 40 °C and the detector was a photodiode array (ProStar, Varian). Peaks were detected at 297 nm and analyzed with the software Varian Star LC workstation 6.41. The mobile phase was composed of water and acetonitrile, both solvents with 0.2% (v/v) of formic acid, and the flow rate was 0.8 mL/min. The gradient started with 15% (v/v) of acetonitrile. The acetonitrile percentage was increased to 40% (v/v) within 5 min, keeping this percentage constant during 5 min. After that, the mobile phase returned to the initial conditions and the column was equilibrated for 5 min.

### Purification of Glucosylated Derivatives of Phloretin

The reaction was scaled up to purify the glucosylated products. The reaction mixture contained 100 mg of phloretin in 2 mL of acetone, 6.84 g of sucrose in 17 mL of 50 mM MOPS buffer (pH 6.5) and sucrose phosphorylase TtSPP\_R134A (65 U). The mixture was kept at 48 °C during 56 h with orbital shaking (1000 rpm), and the glucosylation progress was followed by TLC and HPLC as described. When the concentration of the monoglucoside derivative reached a value of approximately 4.3 mg/mL, the reaction was stopped with methanol (20 mL) and the solvent evaporated with a rotary evaporator (model R-

210, Büchi; Flawil, Switzerland). The purification was carried out using a silica gel 60 (particle size 0.06–0.2 mm, Scharlau) chromatographic column after extraction steps of phenolic compounds with 2-butanone (5 × 20 mL) to remove the residual sugars. The solutions with suspended silica were evaporated with the rotary evaporator and the product was adsorbed in the silica. The mobile phase consisted of a mixture of ethyl acetate, methanol and water at a ratio of 30:5:4 (v/v/v). The different fractions were collected in test tubes and the purification was followed by TLC with the method previously described. Finally, the solvents were evaporated to obtain the pure products.

### Mass Spectrometry (MS)

The molecular weight of purified phloretin glucosides was determined by mass spectrometry with an electrospray coupled to a hybrid QTOF analyzer (model QSTAR, Pulsar i, AB Sciex) in positive reflector mode. Methanol with sodium iodide was used as the ionizing phase.

### Nuclear Magnetic Resonance (NMR) Analysis

The structure of the glucosylated derivatives of phloretin was determined using a combination of 1D and 2D (COSY, DEPT-HSQC, NOESY) standard NMR techniques. The spectra of the samples, dissolved in DMSO-*d*<sub>6</sub> (ca. 7 mM), were recorded on a Bruker IVDr 600 spectrometer equipped with a BBI probe with gradients in the Z axis, at a temperature of 300 K. Chemical shifts were expressed in parts per million (ppm). Residual DMSO-*d*<sub>5</sub> signal was used as an internal reference (2.5 ppm). All the employed pulse sequences were provided by Bruker. For the DEPT-HSQC experiment, values of 8 ppm and 1 K points, for the <sup>1</sup>H dimension, and 165 ppm and 256 points for the <sup>13</sup>C dimension, were used. For the homonuclear COSY and NOESY experiments, 8 ppm windows were used with a 1 K × 256 point matrix. For the NOESY the mixing time was 500 ms.

### Phloretin 4'-O- $\alpha$ -D-Glucopyranoside (1)

The compound (1) was obtained as a pinkish powder (58.3 mg, 33%); <sup>1</sup>H NMR (CD<sub>3</sub>OD)  $\delta$ : 2.86 (2H, m, CH<sub>2</sub>- $\beta$ ), 3.30 (2H, m, CH<sub>2</sub>- $\alpha$ ), 3.45 (1H, dd, J = 8.94, 9.96 Hz, H4''), 3.54 (1H, ddd, J = 2.58, 4.38, 9.96 Hz, H5''), 3.57 (1H, dd, J = 3.63, 9.75 Hz, H2''), 3.70 (1H, dd, J = 4.35, 12.15 Hz, H6''a), 3.74 (1H, dd, J = 2.58, 12.06 Hz, H6''b), 3.81 (1H, dd, J = 9.09, 9.57 Hz, H3''), 5.53 (1H, d, J = 3.60 Hz, H1''), 6.17 (2H, s, H3'/H5'), 6.69 (2H, d, J = 8.50 Hz, H2/H6), 7.04 (2H, d, J = 8.50 Hz, H3/H5); <sup>13</sup>C NMR (CD<sub>3</sub>OD)  $\delta$ : 31.2 (CH<sub>2</sub>  $\beta$ ), 47.4 (CH<sub>2</sub>  $\alpha$ ), 62.0 (C6''), 71.0 (C4''), 73.0 (C2''), 74.6 (C5''), 74.8 (C3''), 96.4 (C3'/C5'), 98.4 (C1''), 107.0 (C1'), 115.9 (C3/C5), 130.3 (C2/C6), 133.8 (C1), 156.6 (C4), 164.5 (C4'), 165.7 (C2'/C6'), 207.3 (CO); HPLC-UV (297 nm): *t*<sub>R</sub> 9.36 min (90%); ESI-MS (*m/z*) 459.1264 [M + Na]<sup>+</sup>.

### Phloretin 4'-O-[ $\alpha$ -D-Glucopyranosil-(1 $\rightarrow$ 3)-O- $\alpha$ -D-Glucopyranoside] (2)

Column chromatography on silica gel afforded the compound (2) as an orange powder (16.2 mg, 6%); <sup>1</sup>H NMR (CD<sub>3</sub>OD)  $\delta$ :

2.86 (2H, m, CH<sub>2</sub>- $\beta$ ), 3.30 (2H, m, CH<sub>2</sub>- $\alpha$ ), 3.29 (1H, H4'''), 3.47 (1H, H2'''), 3.58 (1H, H5'''), 3.74–3.64 (6H, H3''', H2'', H4'', 2H6''', H6''), 3.8 (1H, H6''), 3.91 (1H, H3''), 3.96 (1H, H5'''), 5.22 (1H, d, J = 3.70 Hz, H1'''), 5.57 (1H, d, J = 3.70 Hz, H1''), 6.18 (2H, s, H3'/H5'), 6.69 (2H, d, J = 8.50 Hz, H2/H6), 7.04 (2H, d, J = 8.50 Hz, H3/H5); HPLC-UV (297 nm): *t*<sub>R</sub> 9.14 min (80%). ESI-MS (*m/z*) 621.1787 [M + Na]<sup>+</sup>.

### Automated Docking of Different Phloretin Glucosides into TtSPP\_R134A Structure

The three putative phloretin monoglucosylated ligands were built using PyMolX11Hybrid (The PyMOL Molecular Graphics System, Version 2.0 Schrödinger, LLC).<sup>[44]</sup> The coordinates of TtSPP<sup>[23b]</sup> (PDB code 6S9 V) were modified to R148A mutation in Coot.<sup>[45]</sup> R148 residue in crystal structure deposited in the PDB database corresponds to R134 in wild-type TtSPP sequence due to 14 residues long N-terminal (histidine) tag. All other molecules and water found in the crystal were removed, and this protein was used as a receptor in the docking simulation. AutodockTools<sup>[33]</sup> was used to prepare the coordinates and the ligands to create the .pdbqt files. Polar hydrogens and charges (computed Gasteiger method) were added to the receptor coordinates, and these coordinates were treated as rigid side chain residues. The glycosidic linkages between the glucose and phloretin, and the four C–C bonds linking the two aromatic rings in the phloretin molecule were defined as rotatable bonds in the different complexes. Firstly, a grid box was manually defined to run Autogrid, and Autodock 4.2<sup>[33]</sup> was used for a preliminary docking simulation to find the best phloretin glycosylation position. Autodock 4.2 was executed with the Lamarckian genetic algorithm, and 25 possible conformations were calculated for each monoglucoside derivative. A population size of 150, rate of gene mutation 0.02, and crossover rate of 0.8 were the standard parameters chosen to launch the program. Most consistent results were obtained for the para- derivative (position a) above of the glucose molecule in the triphenolic ring, which presents a clearly preferred first ranked cluster with minimum –7.5 Kcal/mol binding energy (Figure S6). Therefore, assuming a *p*-derivative as the main glucosylated product, AutoDock Vina program<sup>[34]</sup> was then used to improve the accuracy of the docking method, and several residues protruding at the catalytic tunnel, were defined as a flexible side chain in AutoDock Tools. The grid box around the catalytic pocket was defined with 30 Å × 30 Å × 60 Å dimensions. Exhaustiveness was adjusted to 1000 and calculations for the docking were performed with Lamarckian Genetic Algorithm. Around 20 solutions were calculated in a binding energy range between –12.6 and –11.6 Kcal/mol. The best solutions were selected through an energetic and conformational criterion.

### Solubility of Phloretin and its Glucosides

Aqueous solutions of phloretin and the corresponding  $\alpha$ -glucosides were maintained at 25 °C during 3 days in water at saturated conditions with orbital stirring. The samples were centrifuged and the supernatant solution was diluted in methanol to fit the calibration curve of phloretin (0–200  $\mu$ g/mL). Different volumes of 200  $\mu$ L of each sample were taken



by triplicate, and the absorbance was measured by UV spectrophotometry (Tecan Infinite M200) at 297 nm.

### Antioxidant Activity

The antioxidant activity was determined with the 2,2-diphenyl-1-picrylhydrazyl (DPPH) and the 2,2-azino-bis(3-ethylbenzothiazoline-6-sulfonic acid) diammonium salt (ABTS) method, using Trolox as reference antioxidant compound. The DPPH and ABTS assays were performed by triplicate in 96-well plates. The significant differences between the values were calculated with a *t-test* comparing the average and their standard deviations, considering *n* the number of experiments and significant differences when  $p < 0.025$ .

**DPPH assay.** A solution of 200  $\mu\text{M}$  of DPPH was made in methanol. Different dilutions of each antioxidant in methanol were made depending on the antioxidant capacity. For Trolox, the maximum concentration was 100  $\mu\text{M}$ . For phloretin and their glucosides the concentrations were between 0 and 500  $\mu\text{M}$ . The assay was adapted to a 96-well plate. A volume of 100  $\mu\text{L}$  of each antioxidant was taken and 200  $\mu\text{L}$  of DPPH solution was added. The plate was incubated in the dark for 15 min at room temperature. Next, the absorbance was measured with a Zenyth 200 spectrophotometer at 540 nm. The EC50 was defined as the concentration of compound needed to reduce the DPPH absorbance to 50%. The results were also expressed as Trolox Equivalent Antioxidant Capacity (TEAC), which corresponds to the concentration of the active compound ( $\mu\text{M}$ ) that reduces the absorbance of DPPH the same that 1  $\mu\text{M}$  of Trolox. The TEAC value was calculated from EC50 of each compound and EC50 of Trolox.

**ABTS assay.** The working solution was prepared by mixing 5 ml of ABTS (7 mM) with 5 mL of potassium persulfate  $\text{K}_2\text{S}_2\text{O}_8$  (2.45 mM) and leaving it in the dark during 16 h at room temperature to oxidize the ABTS to the cation radical  $\text{ABTS}^{\bullet+}$ . Standard solutions with concentrations between 0 and 200  $\mu\text{M}$  for Trolox and between 0 and 1000  $\mu\text{M}$  for phloretin and its glucosides were prepared in methanol. The antioxidants (20  $\mu\text{L}$ ) at different concentrations were mixed with 230  $\mu\text{L}$  of  $\text{ABTS}^{\bullet+}$  working solution (previously diluted with methanol to get an absorbance of 0.7 at 655 nm). After incubation in the dark at room temperature, the absorbance was measured with a Zenyth 200 spectrophotometer at 655 nm to get the linear regressions of the antioxidants. The EC50 was referred to the concentration of compound needed to reduce the  $\text{ABTS}^{\bullet+}$  absorbance to 50%. The results were also expressed as Trolox Equivalent Antioxidant Capacity (TEAC) as described in the DPPH assay, calculated from EC50 of each compound and EC50 of Trolox.

### Percutaneous Activity Methodology

The *in vitro* release study was carried out with pig biopsies placed on Franz static diffusion cells (3 mL, 1.86  $\text{cm}^2$  of exposed area, diameter: 30 mm, Lara-Spiral, Courtenon, France) in order to determine the compartmental distribution of Active Pharmaceutical Ingredient (API) after an exposure time of 24 h. The OECD Guidelines were closely adhered to during this study.<sup>[46]</sup> The pig skin, provided by the Department of

Cardiology of the Hospital Clinic (Barcelona, Spain), is considered morphologically and functionally equivalent to human skin for percutaneous absorption studies.<sup>[47]</sup> The procedure for these studies was described in previous reports.<sup>[41]</sup> Ultra-pure water was employed as receptor fluid, and cells were placed in a thermostated water bath (32 °C) containing a magnetic stirring device to obtain the skin surface temperature at  $32 \pm 1$  °C. The integrity of the skin samples was evaluated by measuring the transepidermal water loss (TEWL) with Tewameter TM300 (Courage & Khazaka, Cologne, Germany) considering correct TEWL values under  $15 \text{ gm}^{-2} \text{ h}^{-1}$ . Solutions with active compound (phloretin and its glucosides) were applied (10.75  $\mu\text{L}/\text{cm}^2$ ) on dermatomized porcine skin biopsies. Experiments were done by triplicate in three diffusion cells, and an extra diffusion cell without any active compound was used as control. After 24 h, the skin surface was washed to recover the excess of compounds (W). Then, the receptor fluid (RF) was recovered, and stripping procedures were performed on the surface horny layers of the stratum corneum (SC) with adhesive tape (D-squame, Cuderm Corporation, Dallas, USA). Eight strips were employed in order to remove most of the amount of substance contained in the stratum corneum. The viable epidermis (E) was separated from the dermis (D) after heat treatment. The different samples to be analyzed (W, RF, SC, E and D) were extracted and/or diluted in methanol (Merck, Darmstadt, Germany). The phloretin and the corresponding glucosides concentrations were analyzed by HPLC, as previously described. The substance is considered absorbed when is present in epidermis (except for the stratum corneum), dermis and receptor fluid. The amounts founded in the stratum corneum are not considered to be percutaneously absorbed.<sup>[46c]</sup> The results are shown as mean values (expressed as  $\mu\text{g}/\text{cm}^2$ )  $\pm$  standard deviations. The Kruskal-Wallis test was applied for group comparisons, with the software STATGRAPHICS<sup>®</sup>, assuming significant differences when  $p < 0.05$ .

### Acknowledgements

We thank Manuel Ferrer and David Almendral (ICP-CSIC) for the enzyme production support. The authors would like to express their gratitude to the members of Center of Synthetic Biology, specially Koen Beerens, Jorick Franceus, Stevie Van Overtveldt, Ophelia Gevaert, Matthieu Da Costa, Shari Dhaene, Marc De Doncker, Emma De Beul, Gilles Velghe, Dries Duchi, José Manuel Salvador López, Mónica Texido and Alba López for their constructive suggestions, discussions and all help received. We thankfully acknowledge the NMR resources and the technical support provided by the Laboratorio de RMN de Euskadi (LRE) of the Spanish ICTS Red de Laboratorios de RMN de Biomoléculas (R-LRB). This work was supported by grants from the Spanish Ministry of Economy and Competitiveness (Grants BIO2016-76601-C3-1,3-R and PID2019-105838RB-C31). We thank the support of the scholarship of Jose Luis Gonzalez from Spanish Ministry of Education, Culture and Sport through the National Program FPU (FPU17/00044) and for the help received to do the stay at Ghent University with the subprogram for mobility aids FPU 2018. The present work could not be performed without the collaboration and Contribution of the Service of Dermocosmetic Assessment from IQAC-CSIC.

## References


- [1] a) Y. Z. Fang, S. Yang, G. Y. Wu, *Nutrition* **2002**, *18*, 872–879; b) P. Poprac, K. Jomova, M. Simunkova, V. Kollar, C. J. Rhodes, M. Valko, *Trends Pharmacol. Sci.* **2017**, *38*, 592–607.
- [2] a) B. Zhou, Z. L. Liu, *Pure Appl. Chem.* **2005**, *77*, 1887–1903; b) G. Mantovani, A. Maccio, C. Madeddu, L. Mura, G. Gramignano, M. R. Lusso, V. Murgia, P. Camboni, L. Ferrel, M. Mocchi, E. Massa, *Free Radical Res.* **2003**, *37*, 213–223; c) F. Gaboriau, J. G. Delcros, J. P. Moulinoux, *J. Pharmacol. Toxicol. Methods* **2002**, *47*, 33–43; d) E. B. Mojzer, M. K. Hrnčič, M. Škerget, Ž. Knez, U. Bren, *Molecules* **2016**, *21*, 901.
- [3] a) R. R. Hou, J. Z. Chen, H. Chen, X. G. Kang, M. G. Li, B. R. Wang, *Cell Biol. Int.* **2008**, *32*, 22–30; b) N. A. Singh, A. K. A. Mandal, Z. A. Khan, *Nutr. J.* **2016**, *15*; c) D. V. Ratnam, D. D. Ankola, V. Bhardwaj, D. K. Sahana, M. N. V. R. Kumar, *J. Controlled Release* **2006**, *113*, 189–207; d) O. I. Aruoma, J. P. E. Spencer, D. Warren, P. Jenner, J. Butler, B. Halliwell, *Food Chem.* **1997**, *60*, 149–156; e) E. J. Seo, N. Fischer, T. Efferth, *Pharmacol. Res.* **2018**, *129*, 262–273; f) K. W. Lange, S. Li, *BioFactors* **2018**, *44*, 83–90; g) S. Schaffer, H. Asseburg, S. Kuntz, W. E. Muller, G. P. Eckert, *Mol. Neurobiol.* **2012**, *46*, 161–178; h) J. L. Gonzalez-Alfonso, P. Peñalver, A. O. Ballesteros, J. C. Morales, F. J. Plou, *Front. Nutr.* **2019**, *6*:30.
- [4] N. A. Nguyen, N. T. Cao, T. H. H. Nguyen, T. K. Le, G. S. Cha, S. K. Choi, J. G. Pan, S. J. Yeom, H. S. Kang, C. H. Yun, *Pharmaceuticals* **2020**, *13*, 1–14.
- [5] a) X. Shen, L. Wang, N. Zhou, S. Gai, X. Liu, S. Zhang, *Food Funct.* **2020**, *11*, 392–403; b) A. Takeno, I. Kanazawa, M. Notsu, K.-i. Tanaka, T. Sugimoto, *Am. J. Physiol. Endocrinol. Metab.* **2018**, *314*, E115–E123.
- [6] Y. H. Hsiao, M. J. Hsieh, S. F. Yang, S. P. Chen, W. C. Tsai, P. N. Chen, *Phytomedicine* **2019**, *62*.
- [7] S. Yin, X. Zhang, F. Lai, T. Liang, J. Wen, W. Lin, J. Qiu, S. Liu, L. Li, *FEBS Lett.* **2018**, *592*, 2361–2377.
- [8] a) V. Crespy, O. Aprikian, C. Morand, C. Besson, C. Manach, C. Demigné, C. Rémésy, *J. Nutr.* **2001**, *131*, 3227–3230; b) Y. Wang, D. Li, H. Lin, S. Jiang, L. Han, S. Hou, S. Lin, Z. Cheng, W. Bian, X. Zhang, Y. He, K. Zhang, *Food Sci. Nutr.* **2020**, *8*, 3545–3558.
- [9] P. Monge, E. Solheim, R. R. Scheline, *Xenobiotica* **1984**, *14*, 917–924.
- [10] J. Zhao, J. Yang, Y. Xie, *Int. J. Pharm.* **2019**, *570*.
- [11] a) B. D. Arbo, C. André-Miral, R. G. Nasre-Nasser, L. E. Schimith, M. G. Santos, D. Costa-Silva, A. L. Muccillo-Baisch, M. A. Hort, *Front. Aging Neurosci.* **2020**, *12*; b) N. Ilmberger, U. Rabausch, in *Methods Mol. Biol.* **2017**, *1539*, 229–236.
- [12] L. Xu, T. Qi, L. Xu, L. Lu, M. Xiao, *J. Carbohydr. Chem.* **2016**, *35*, 1–23.
- [13] a) L. Weignerova, V. Kren, *Top. Curr. Chem.* **2010**, *295*, 121–146; b) J. Vrba, V. Kren, J. Vacek, B. Papouskova, J. Ulrichova, *Phytother. Res.* **2012**, *26*, 1746–1752; c) P. C. H. Hollman, M. N. C. P. Buijsman, Y. Van Game-  
ren, E. P. J. Cnossen, J. H. M. De Vries, M. B. Katan, *Free Radical Res.* **1999**, *31*, 569–573; d) V. Kren, L. Martinkova, *Curr. Med. Chem.* **2001**, *8*, 1303–1328.
- [14] T. Makino, R. Shimizu, M. Kanemaru, Y. Suzuki, M. Moriwaki, H. Mizukami, *Biol. Pharm. Bull.* **2009**, *32*, 2034–2040.
- [15] a) T. Raab, D. Barron, F. Arce Vera, V. Crespy, M. Oliveira, G. Williamson, *J. Agric. Food Chem.* **2010**, *58*, 2138–2149; b) A. Lepak, A. Gutmann, S. T. Kulmer, B. Nidetzky, *ChemBioChem* **2015**, *16*, 1870–1874.
- [16] T. Desmet, W. Soetaert, *Biocatal. Biotransform.* **2011**, *29*, 1–18.
- [17] B. Henrissat, G. J. Davies, *Plant Physiol.* **2000**, *124*, 1515–1519.
- [18] a) N. Miguez, M. Ramirez-Escudero, M. Gimeno-Perez, A. Poveda, J. Jimenez-Barbero, A. O. Ballesteros, M. Fernandez-Lobato, J. Sanz-Aparicio, F. J. Plou, *Chem-CatChem* **2018**, *10*, 4878–4887; b) J. A. Méndez-Liter, I. Tundidor, M. Nieto-Dominguez, B. F. De Toro, A. González Santana, L. I. De Eugenio, A. Prieto, J. L. Asensio, F. J. Cañada, C. Sánchez, M. J. Martínez, *Microb. Cell Fact.* **2019**, *18*, 97; c) K. Z. G. Ara, S. Khan, T. S. Kulkarni, T. Pozzo, E. N. Karlsson, *Adv. Enzyme Biotechnol.* **2013**, *9*–21; d) E. Karnišová Potocká, M. Mastihubová, V. Mastihuba, *Biocatal. Biotransform.* **2018**, *37*, 1–7.
- [19] a) L. T. Tran, V. Blay, S. Luang, C. Eurtivong, S. Choknud, H. González-Díaz, J. R. Ketudat Cairns, *Green Chem.* **2019**, *21*, 2823–2836; b) F. J. Plou, A. Gómez de Segura, A. Ballesteros, in *Industrial enzymes: Structure, Function and Application* (Eds.: J. Polaina, A. P. MacCabe), Springer, New York, **2007**, pp. 141–157.
- [20] a) D. M. Liang, J. H. Liu, H. Wu, B. B. Wang, H. J. Zhu, J. J. Qiao, *Chem. Soc. Rev.* **2015**, *44*, 8350–8374; b) J. Seibel, H. J. Jördening, K. Buchholz, *Biocatal. Biotransform.* **2006**, *24*, 311–342.
- [21] M. Klimacek, A. Sigg, B. Nidetzky, *Biotechnol. Bioeng.* **2020**, *117*, 2933–2943.
- [22] A. Percy, H. Ono, K. Hayashi, *Carbohydr. Res.* **1998**, *308*, 423–429.
- [23] a) Y. Li, Z. Li, X. He, L. Chen, Y. Cheng, H. Jia, M. Yan, K. Chen, *J. Biotechnol.* **2019**, *305*, 27–34; b) J. Franceus, N. Capra, T. Desmet, A. M. W. H. Thunnissen, *Int. J. Mol. Sci.* **2019**, *20*; c) K. De Winter, T. Desmet, T. Devlamynck, L. Van Renterghem, T. Verhaeghe, H. Pelantová, V. Křen, W. Soetaert, *Org. Process Res. Dev.* **2014**, *18*, 781–787.
- [24] a) L. Lu, L. Xu, Y. Guo, D. Zhang, T. Qi, L. Jin, G. Gu, L. Xu, M. Xiao, *PLoS One* **2015**, *10*; b) M. Kraus, C. Grimm, J. Seibel, *Chem. Commun.* **2017**, *53*, 12181–12184.
- [25] M. E. Dirks-Hofmeister, T. Verhaeghe, K. De Winter, T. Desmet, *Angew. Chem.* **2015**, *54*, 9289–9292.
- [26] K. De Winter, G. Dewitte, M. E. Dirks-Hofmeister, S. De Laet, H. Pelantová, V. Křen, T. Desmet, *J. Agric. Food Chem.* **2015**, *63*, 10131–10139.

- [27] T. P. Anunciato Casarini, L. A. Frank, A. R. Pohlmann, S. S. Guterres, *Eur. J. Pharmacol.* **2020**, 889.
- [28] a) J. L. González-Alfonso, N. Míguez, J. D. Padilla, L. Leemans, A. Poveda, J. Jiménez-Barbero, A. O. Ballesteros, G. Sandoval, F. J. Plou, *Molecules* **2018**, 23; b) T. Marié, G. Willig, A. R. S. Teixeira, E. Gazaneo Barboza, A. Kotland, A. Gratia, E. Courrot, J. Hubert, J. H. Renault, F. Allais, *ACS Sustainable Chem. Eng.* **2018**, 6, 5370–5380; c) E. Potocká, M. Mastihubová, V. Mastihubová, *J. Mol. Catal. B* **2015**, 113, 23–28; d) J. L. Gonzalez-Alfonso, L. Leemans, A. Poveda, J. Jiménez-Barbero, A. Olmo Ballesteros, F. J. Plou, *J. Agric. Food Chem.* **2018**, 66, 7402–7408; e) L. S. Mazzaferro, G. Weiz, L. Braun, M. Kotik, H. Pelantová, V. Křen, J. D. Breccia, *Biotechnol. Appl. Biochem.* **2019**, 66, 53–59.
- [29] a) M. Mikl, A. Dennig, B. Nidetzky, *J. Biotechnol.* **2020**, 322, 74–78; b) K. Schmölzer, M. Lemmerer, B. Nidetzky, *Biotechnol. Bioeng.* **2018**, 115, 545–556; c) L. Bungaruang, A. Gutmann, B. Nidetzky, *Adv. Synth. Catal.* **2013**, 355, 2757–2763.
- [30] a) C. Wen, W. Huang, M. M. He, W. L. Deng, H. H. Yu, *Biotechnol. Lett.* **2020**, 42, 135–142; b) T. Zhang, J. Liang, P. Wang, Y. Xu, Y. Wang, X. Wei, M. Fan, *Sci. Rep.* **2016**, 6, 35692.
- [31] H. Overwin, V. Wray, B. Hofer, *J. Biotechnol.* **2015**, 211, 103–106.
- [32] M. Ramirez-Escudero, N. Míguez, M. Gimeno-Perez, A. O. Ballesteros, M. Fernandez-Lobato, F. J. Plou, J. Sanz-Aparicio, *Sci. Rep.* **2019**, 9, 17441.
- [33] A. R. Allouche, *J. Comput. Chem.* **2011**, 32, 174–182.
- [34] O. Trott, A. J. Olson, *J. Comput. Chem.* **2010**, 31, 455–461.
- [35] O. Mirza, L. K. Skov, D. Sprogøe, L. A. M. Van Den Broek, G. Beldman, J. S. Kastrup, M. Gajhede, *J. Biol. Chem.* **2006**, 281, 35576–35584.
- [36] a) D. K. Vivekanandhan, P. R. P. Verma, S. K. Singh, *Curr. Nutr. Food Sci.* **2016**, 12, 12–22; b) G. Núñez-López, A. Herrera-González, L. Hernández, L. Amaya-Delgado, G. Sandoval, A. Gschaedler, J. Arrizon, M. Remaud-Simeon, S. Morel, *Enzyme Microb. Technol.* **2019**, 122, 19–25.
- [37] J. González-Alfonso, D. Rodrigo-Frutos, E. Belmonte-Reche, P. Peñalver, A. Poveda, J. Jiménez-Barbero, A. Ballesteros, Y. Hirose, J. Polaina, J. Morales, M. Fernández-Lobato, F. Plou, *Molecules* **2018**, 23, 1271.
- [38] P. Torres, A. Poveda, J. Jimenez-Barbero, J. L. Parra, F. Comelles, A. O. Ballesteros, F. J. Plou, *Adv. Synth. Catal.* **2011**, 353, 1077–1086.
- [39] a) A. M. Aura, K. A. O'Leary, G. Williamson, M. Ojala, M. Bailey, R. Puupponen-Pimiä, A. M. Nuutila, K. M. Oksman-Caldentey, K. Poutanen, *J. Agric. Food Chem.* **2002**, 50, 1725–1730; b) S. Pathak, P. Kesavan, A. Banerjee, A. Banerjee, G. S. Celep, L. Bissi, F. Marotta, in *Polyphenols: Mechanisms of Action in Human Health and Disease* (Eds.: V. R. Preedy, S. Zibadi, R. Watson), Academic Press, Cambridge, MA, **2018**, pp. 347–359; c) A. Braune, M. Blaut, *Gut Microbes* **2016**, 7, 216–234; d) A. L. A. Sesink, I. C. W. Arts, M. Faassen-Peters, P. C. H. Hollman, *J. Nutr.* **2003**, 133, 773–776; e) I. C. W. Arts, A. L. A. Sesink, M. Faassen-Peters, P. C. H. Hollman, *Brit. J. Nutr.* **2004**, 91, 841–847.
- [40] a) C. Oresajo, T. Stephens, P. D. Hino, R. M. Law, M. Yatskayer, P. Foltis, S. Pillai, S. R. Pinnell, *J. Cosmet. Dermatol.* **2008**, 7, 290–297; b) H. Kum, K. B. Roh, S. Shin, K. Jung, D. Park, E. Jung, *Int. J. Cosmet. Sci.* **2016**, 38, 85–92; c) S. Shin, H. Kum, D. Ryu, M. Kim, E. Jung, D. Park, *Int. J. Mol. Sci.* **2014**, 15, 18919–18940.
- [41] C. Alonso, L. Rubio, S. Touriño, M. Martí, C. Barba, F. Fernández-Campos, L. Coderch, J. L. Parra, *Free Radical Biol. Med.* **2014**, 75, 149–155.
- [42] a) C. Alonso, M. Martí, C. Barba, V. Carrer, L. Rubio, L. Coderch, *Arch. Dermatol. Res.* **2017**, 309, 423–431; b) C. Alonso, M. Martí, C. Barba, M. Lis, L. Rubio, L. Coderch, *J. Photochem. Photobiol. B* **2016**, 156, 50–55; c) C. Alonso, R. Lucas, C. Barba, M. Martí, L. Rubio, F. Comelles, J. C. Morales, L. Coderch, J. L. Parra, *J. Pharm. Pharmacol.* **2015**, 67, 900–908.
- [43] S. Waffenschmidt, L. Jaenicke, *Anal. Biochem.* **1987**, 165, 337–340.
- [44] W. L. DeLano, *CCP4 Newsletter on Protein Crystallography*, 40, 1–8.
- [45] P. Emsley, K. Cowtan, *Acta Crystallogr. Sect. D* **2004**, 60, 2126–2132.
- [46] a) *Skin absorption: In vitro method. OECD Guideline for the testing of chemicals. Guideline 428*, Paris, **2004**; b) *Guidance document for the conduct of skin absorption studies. OECD series on testing and assessment. Guidance 28*, Paris, **2004**; c) *Basic criteria for the in vitro assessment of percutaneous absorption of cosmetic ingredients. SCCNFP/0690*, **2003**; d) H. Schaefer, T. E. Redelmeier, *Skin Barrier: Principles of Percutaneous Absorption*, Karger, Basel, **1996**; e) A. C. Williams, *Transdermal and topical drug delivery*, Pharmaceutical Press, London, **2003**.
- [47] G. M. Gray, H. J. Yardley, *J. Lipid Res.* **1975**, 16, 434–440.

## RESEARCH ARTICLE

Enzymatic Synthesis of Phloretin  $\alpha$ -Glucosides Using a Sucrose Phosphorylase Mutant and its Effect on Solubility, Antioxidant Properties and Skin Absorption

*Adv. Synth. Catal.* **2021**, *363*, 1–12

 J. L. Gonzalez-Alfonso, Z. Ubiparip, E. Jimenez-Ortega, A. Poveda, C. Alonso, L. Coderch, J. Jimenez-Barbero, J. Sanz-Aparicio, A. O. Ballesteros, T. Desmet\*, F. J. Plou\*

